Eksergi
Chemical Engineering Journal
Vol 23, No. 1. 2026

ISSN: 1410-394X
e-ISSN: 2460-8203

# Catalytic Disproportionation of Indonesian Gum Rosin over Pd/C: Isomerization Pathways of Merkusic Acid

Meiga Putri Wahyu Hardhianti *

*Department of Chemical Engineering, Faculty of Engineering, Universitas Gadjah Mada, Jl. Grafika No. 2, Yogyakarta 55281, Indonesia*

**Article history:**

Submitted 28 October 2025
Revision 6 November 2025
Accepted 19 December 2025
Online 15 January 2026

**ABSTRACT**: Indonesian gum rosin is a renewable natural resource with a unique composition characterized by the presence of merkusic acid. This study investigates its catalytic disproportionation over a Pd/C catalyst in a sealed batch reactor at 200 °C and 240 °and to qualitatively assess its reactivity based on product distribution observed by GC–MS. The reaction products were analyzed using FTIR and GC–MS after methylation. Abietic acid was observed to be among the more reactive resin acids, undergoing typical disproportionation pathways inferred from GC–MS peak changes, including hydrogenated (e.g., dihydroabietic) and dehydrogenated (dehydroabietic) derivatives. The formation of dehydroabietic acid was more prominent at 200 °C, while at 240 °C the GC–MS profiles suggest increased contributions from hydrogenation and isomerization side reactions. In contrast, merkusic acid showed a distinct transformation profile, undergoing preferential double-bond isomerization inferred from the appearance of structural isomers with identical molecular ions (m/z 364). These findings provide semi-quantitative, GC–MS-based insights into the temperature-dependent transformation trends of major resin acids and highlight the distinct isomerization-dominated transformation of merkusic acid in Indonesian gum rosin.

**Keywords:** gum rosin; disproportionation; resin acids; merkusic acid; Pd/C catalyst

## 1. Introduction

Rosin (colophony) is a brittle and semi-transparent solid obtained as a non-volatile residue after pine resin distillation. It mainly comprises diterpenoid monocarboxylic acids (90–95%), known as resin acids, with a minor portion of neutral compounds (Kugler et al., 2019; Maiti et al., 1989; Silvestre & Gandini, 2008). Commercially, rosin is classified as gum rosin (from living pine trees), wood rosin (from pine stumps), and tall oil rosin (from the kraft pulping process). Gum rosin usually contains the highest fraction of abietane-type resin acids, such as abietic acid ($C_{19}H_{29}COOH$), whose conjugated double bonds provide high chemical reactivity (Kugler et al., 2019).

The chemical reactivity of rosin, primarily derived from its carboxylic acid functionality and unsaturated carbon skeleton, enables a wide range of chemical transformations aimed at improving its properties and broadening its industrial applications. One common route is esterification with polyhydric alcohols such as glycerol or pentaerythritol (Hardhianti et al., 2022; Hartanto et al., 2021; Ladero et al., 2012; Zhang et al., 2017), forming rosin esters that are extensively used in adhesives, inks, and coating formulations (Comyn, 1994; Pathak & Dorle, 1987; Xu et al., 2019). Another key modification is catalytic disproportionation, an established industrial process that converts reactive resin acids, particularly abietic acid, into more stable hydrogenated (e.g., dihydroabietic acid) and dehydrogenated (dehydroabietic acid) derivatives (Gu et al., 2020; Kumar et al., 2018; Mostafalu et al., 2017; Souto et al., 2011; Wang et al., 2009, 2013). This transformation markedly enhances the thermal and oxidative stability of rosin, thus enabling its use in higher-value applications.

The catalytic disproportionation of rosin has been widely studied as an effective method to improve its chemical stability and color. Palladium on carbon (Pd/C) is known to catalyze the concurrent hydrogenation and dehydrogenation of abietane-type resin acids, with temperature and catalyst loading strongly influencing product selectivity (Souto et al., 2011; Wang et al., 2009, 2013). Moderate temperatures around 200–220 °C favor the formation of dehydroabietic acid, while higher temperatures promote hydrogenation and isomerization side reactions. Recent studies have also explored alternative hydrogen-transfer catalysts that follow similar mechanistic behavior (Souto et al., 2024).

Indonesia is among the world's leading producers of gum rosin and is distinguished by its relatively high content of merkusic acid, a diterpenoid resin acid rarely found in significant quantities in rosins from other regions such as

* Corresponding Author
Email address: meiga.p.w@ugm.ac.id

China or Brazil (Tanaka et al., 2008; Wiyono et al., 2006). Merkusic acid differs structurally from the more common abietic acid. Merkusic acid has a labdane-type bicyclic skeleton with a bulky exocyclic methylene group, whereas abietic acid has a more planar abietane skeleton with conjugated double bonds. These structural differences increase steric hindrance and may hinder the planar adsorption geometry required for Pd-assisted dehydrogenation.

Despite the abundance of studies on rosin disproportionation, previous work has focused almost exclusively on abietane- and pimarane-type resin acids. The behavior of region-specific components, such as merkusic acid. It is present in high concentrations only in Indonesian Pinus merkusii rosin and has not been systematically investigated.

In this work, the catalytic disproportionation of Indonesian gum rosin over a Pd/C catalyst was investigated, with emphasis on examining how the presence of merkusic acid may influence the observed reaction pathways and product distribution as inferred from GC–MS data. The products were analyzed using Fourier-transform infrared (FTIR) spectroscopy and gas chromatography–mass spectrometry (GC–MS). This study provides qualitative, GC–MS-based insight into the transformation pathways of resin acids in Indonesian gum rosin, an aspect that has not been explicitly discussed in previous reports.

## 2. Materials and Methods

### 2.1. Materials

The materials used in this study included gum rosin obtained from PAK Trenggalek, Indonesia (acid value of 190 mg KOH/g), Pd/C catalyst (5 wt.% palladium on carbon, Sigma Aldrich), trimethylsulfonium hydroxide solution (TMSH) (0.24 M in methanol, Sigma Aldrich), tetrahydrofuran (THF) (99.8%, Merck), and magnesium sulfate anhydrous (99.5%, Sigma Aldrich).

### 2.2. Disproportionation of Gum Rosin

Disproportionation reactions were conducted in a Parr autoclave reactor equipped with a mechanical stirrer and temperature controller to maintain precise reaction conditions. Before each experiment, the reactor was purged several times with nitrogen gas to remove residual oxygen and establish an inert atmosphere. After purging, no additional nitrogen overpressure was applied; the reactor was sealed, and the reaction proceeded at atmospheric pressure. For each reaction, 10 g of gum rosin was mixed with 0.02 g of Pd/C catalyst (0.2 wt.% of the gum rosin mass). The mixture was heated to the target temperatures of 200°C and 240°C, with vigorous stirring at 600 rpm.

A reaction time of 3 hours was selected based on preliminary trials and literature indicating that Pd/C-catalyzed disproportionation reaches a stable product distribution within this duration. A stirring speed of 600 rpm is widely used in heterogeneous catalytic systems of similar viscosity and is sufficient to ensure effective dispersion of the Pd/C catalyst. Each reaction was carried out once under these conditions, and no catalyst recovery or reuse experiments were performed. After completion, the products were cooled to room temperature and stored in sealed vials for analysis.

### 2.3. Characterization of Pd/C Catalyst

$N_2$ adsorption–desorption isotherms of the Pd/C catalyst were measured at 77 K using a Quantachrome NOVA analyzer after degassing at 120 °C for 12 h. The BET method was applied to determine the specific surface area, while the total pore volume and pore size distribution were obtained from the desorption branch using the BJH method.

### 2.4. Characterization of Gum Rosin and Disproportionated Products

The gum rosin and its disproportionated products were characterized by Fourier-transform infrared (FTIR) spectroscopy and gas chromatography–mass spectrometry (GC–MS). FTIR spectra (4000–400 $cm^{-1}$) were recorded to identify functional groups. GC–MS analysis was performed on a Hewlett-Packard 6890/5973 system equipped with a Restek Rxi-5Sil MS column (30 m × 0.25 mm × 0.25 μm). For derivatization, approximately 0.8 mL of the sample solution in THF was mixed with 0.4 mL of TMSH (0.2 M in methanol) and a small amount of anhydrous $MgSO_4$. The mixture was gently vortexed and allowed to stand at room temperature for 3–5 minutes to ensure complete methylation. No heating step was required, as TMSH readily converts carboxylic acids to their corresponding methyl esters under ambient conditions, consistent with standard TMSH derivatization protocols. The absence of underivatized resin acid peaks in the resulting chromatograms confirmed complete methylation.

The derivatized solution was injected into the GC–MS system. The oven temperature program started at 40 °C (held for 0 min), followed by a heating ramp of 10 °C·$min^{-1}$ to 320 °C, giving a total run time of 28 minutes. A split ratio of 100:1 was selected to prevent column overloading due to the high concentration of resin acid derivatives in the samples. Helium was used as the carrier gas at a constant flow of 1.0 mL·$min^{-1}$, and the injector temperature was maintained at 280 °C. Compounds were identified by matching mass spectra with the NIST05a.L library.

## 3. Results and Discussion

### 3.1. Characterisation of Pd/C Catalyst

The textural properties of the Pd/C catalyst were characterized by $N_2$ adsorption–desorption at 77 K. The specific surface area and pore characteristics were determined using BET and BJH methods, respectively. The isotherm exhibited a type IV profile with an H2-type hysteresis loop, indicating a disordered mesoporous structure typical of activated carbon supports. The corresponding textural parameters are summarized in Table 1.

**Table 1.** Textural parameters of the Pd/C catalyst.

| Parameter | Value |
|---|---|

ISSN: 1410-394X
e-ISSN: 2460-8203

| | |
|---|---|
| Specific surface area | 835 $m^2 g^{-1}$ |
| Total pore volume | 0.739 $cm^3 g^{-1}$ |
| Average pore diameter | 3.5 nm |
| Mode pore diameter | 4.0 nm |

The Pd/C catalyst shows a high specific surface area of 835 $m^2 g^{-1}$ and a mesoporous structure, comparable to Pd/C catalysts reported in previous studies on rosin disproportionation, which exhibit BET surface areas in the range of approximately 600–1000 $m^2 g^{-1}$ (Souto et al., 2011; Wang et al., 2009, 2013).

### 3.2. FTIR Analysis of Gum Rosin before and after Disproportionation

The FTIR spectrum of raw gum rosin exhibits a strong C=O stretching band of carboxylic acids at approximately 1695 $cm^{-1}$, accompanied by a broad O–H stretching band in the range of 2500–3300 $cm^{-1}$, which is characteristic of hydrogen-bonded carboxylic acid groups. After disproportionation, the carboxylic acid functionality remains clearly preserved, as evidenced by the persistence of the C=O absorption in the same spectral region. partial modification of the unsaturated resin acid structures.

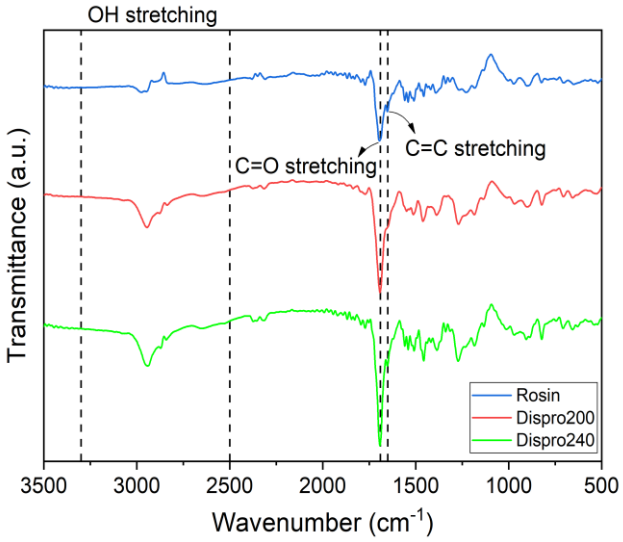


**Figure 1.** FTIR spectra of raw gum rosin (blue line), disproportionation product at 200 °C (red line), and disproportionation product at 240 °C (green line).

No additional absorption band appears in the ester carbonyl region (1735–1750 $cm^{-1}$), indicating that esterification or transesterification side reactions are not detectable under the applied reaction conditions. In contrast, the C=C stretching vibration, observed as a shoulder at approximately 1650 $cm^{-1}$ in the raw rosin spectrum, shows a noticeable decrease in intensity after disproportionation and is retained only as a weak residual band in Dispro240, reflecting

### 3.3. GC–MS Analysis of Gum Rosin and Disproportionated Products

GC–MS analysis was carried out to determine the chemical composition of methylated gum rosin and its disproportionated products (Dispro200 and Dispro240). In the methylated gum rosin, the main components identified were sandaracopimaric acid methyl ester, isopimaric acid methyl ester, methyl dehydroabietate, methyl abietate, neoabietic acid methyl ester, and merkusic acid dimethyl ester (Table 2a).

These compounds are consistent with previous GC–MS analyses of *Pinus merkusii* rosin from Indonesia, which reported abietane- and pimarane-type resin acids together with merkusic acid as characteristic constituents (Wiyono et al., 2006). After disproportionation, additional peaks corresponding to new compounds were detected, including hydrogenated pimarane- and abietane-type acids as well as isomerized merkusic acids (Figure 2b and 2c).

A notable observation is the overlapping peak within the retention time range of 19.55–19.62 min, which contained a mixture of isopimaric acid methyl ester and podocarp-8-en-15-oic acid, 13α-methyl-13-vinyl-, methyl ester. The intensity of this peak decreased in Dispro200 and showed a more drastic reduction in Dispro240 compared to the original rosin, indicating substantial compositional changes during the disproportionation process.

Overall, the chromatographic profiles revealed clear shifts in component distribution: (i) a decrease in the relative intensity of pimarane- and abietane-type acids originally present in gum rosin, (ii) the emergence of new peaks tentatively attributed to hydrogenated and dehydrogenated derivatives, and (iii) the appearance of additional peaks assigned to isomerized merkusic acid dimethyl ester based on consistent retention time and fragmentation pattern changes. These compositional changes are evident in the chromatograms presented in Figure 2 and form the basis for the subsequent discussion of transformation pathways inferred from GC–MS observations.

### 3.4. Reaction Mechanism of Disproportionation

Based on Figure 2d, products derived from pimarane-type acids show clear hydrogenation features. The peak of sandaracopimaric acid methyl ester (RT 19.195) decreases with increasing reaction temperature, while new peaks at RT 19.384 and 19.835 emerge and are tentatively assigned to hydrogenated derivatives. A similar trend is observed for isopimaric acid methyl ester (RT 19.55–19.62), which decreases after reaction, accompanied by peaks at RT 19.765 and 20.115, suggesting the formation of hydrogenated isopimaric/abietic-type acids. These observations are consistent with previous reports on Pd/C-catalyzed disproportionation of rosin (Souto et al., 2011; Wang et al., 2009, 2013).

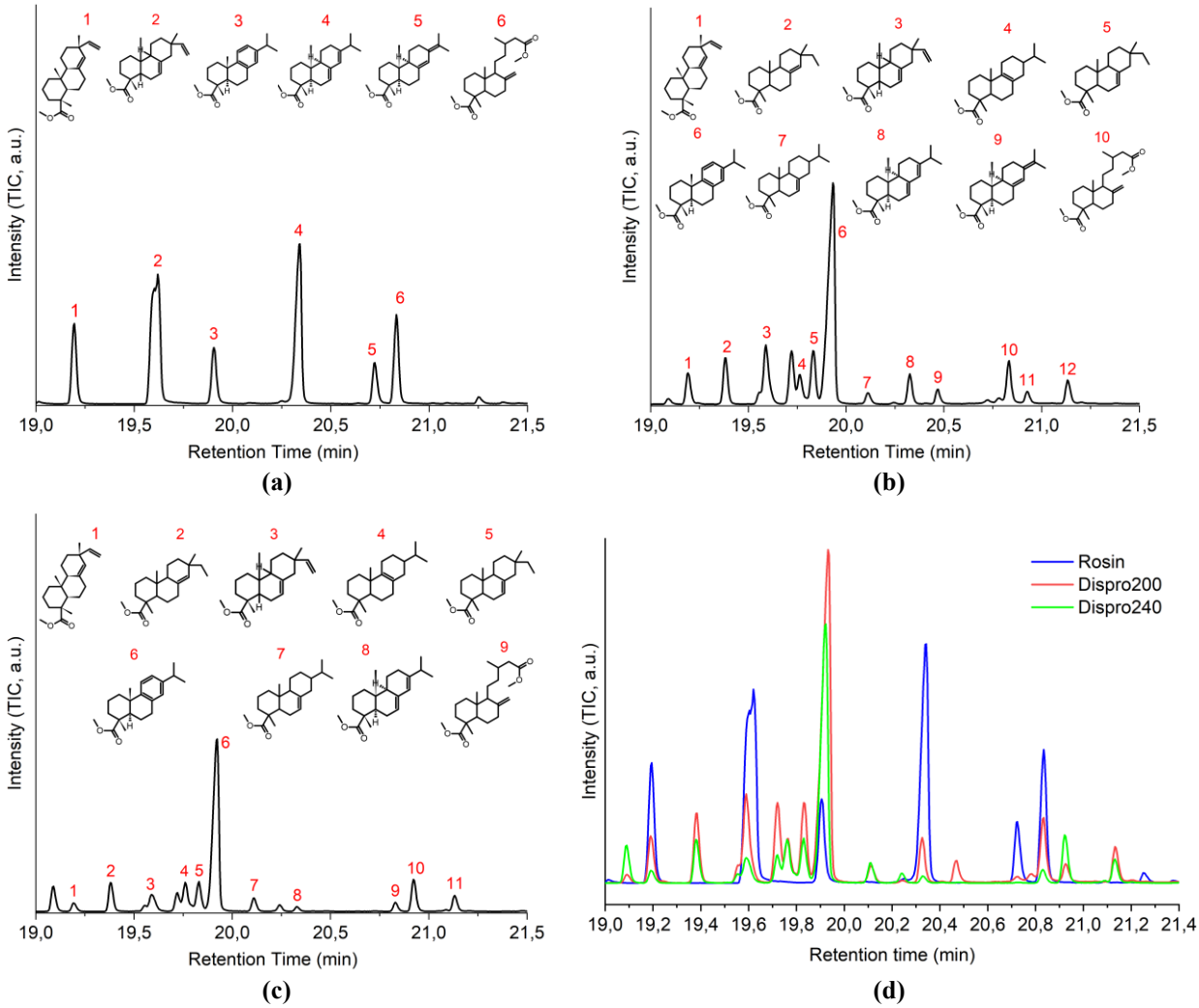


**Figure 2.** Gas chromatography (GC) profiles of methylated samples: (a) raw gum rosin, (b) disproportionation product at 200 °C, (c) disproportionation product at 240 °C, and (d) overlaid chromatograms for direct comparison.

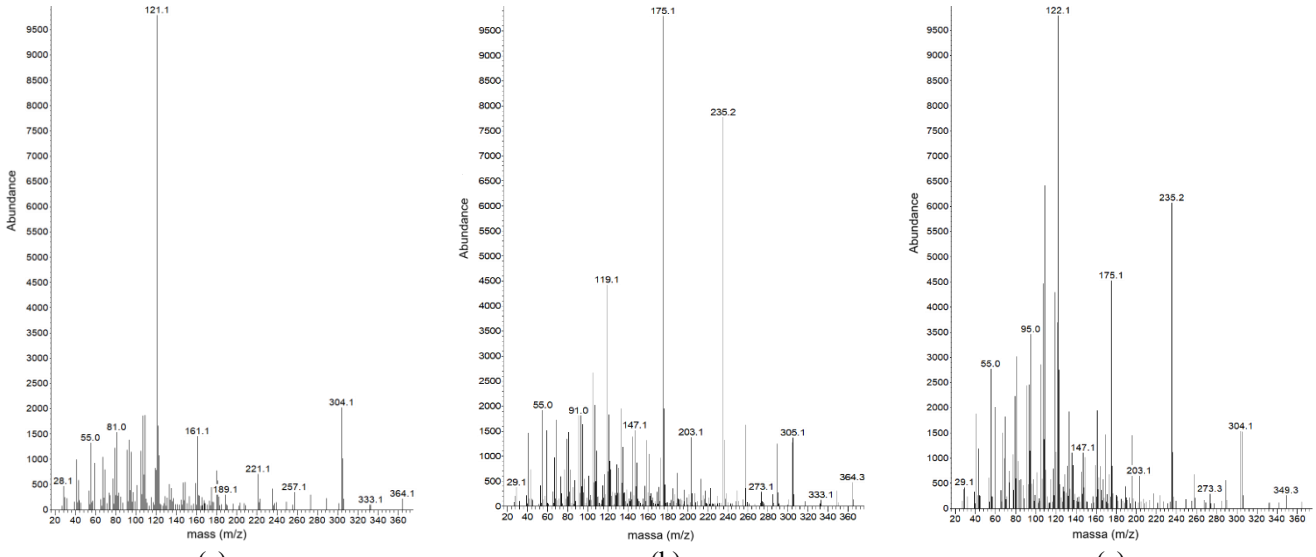


**Figure 3.** Representative mass spectra of the isomerization products from disproportionation product at 240 °C at (a) RT 20.834 min, (b) RT 20.926, and (c) RT 21.132 min, tentatively identified as isomeric merkusic acid dimethyl esters

ISSN: 1410-394X
e-ISSN: 2460-8203

**Table 2.** Chemical composition of methylated gum rosin and its disproportionation products identified by GC-MS. Peak area percentages are semiquantitative and intended for qualitative comparison only.

| Peak | RT | Area Pct* | Compound | CAS | Qual |
|---|---|---|---|---|---|
| | | | **GUM ROSIN** | | |
| 1 | 19.1955 | 4.1816 | Sandaracopimaric acid, methyl ester (Pimarane-type) | 001686-54-0 | 99 |
| 2 | 19.6160 | 12.5715 | Isopimaric acid, methyl ester (Pimarane-type) | 001686-62-0 | 98 |
| 3 | 19.9052 | 3.2408 | Methyl Dehydroabietate (Dehydroabiectic) | 001235-74-1 | 95 |
| 4 | 20.3389 | 10.5096 | Methyl abietate (Abietane-type) | 000127-25-3 | 99 |
| 5 | 20.7245 | 2.2414 | Neoabietic acid, methyl ester (Abietane-type) | 003310-97-2 | 90 |
| 6 | 20.8340 | 4.8683 | Merkusic acid, dimethyl ester | 013902-83-5 | 59 |
| | | | **DISPROPORTIONATION PRODUCT at 200 °C (DISPRO200)** | | |
| 1 | 19.1957 | 1.7353 | Sandaracopimaric acid, methyl ester (Pimarane-type) | 001686-54-0 | 99 |
| 2 | 19.3840 | 2.4246 | Podocarp-8(14)-en-15-oic acid, 13.beta.-ethyl-13-methyl-, methyl ester (Hydrogenated pimarane-type) | 003582-27-2 | 76 |
| 3 | 19.5943 | 4.1812 | Isopimaric acid, methyl ester (Pimarane-type) | 001686-62-0 | 89 |
| 4 | 19.7652 | 1.6454 | Podocarp-8-en-15-oic acid, 13.beta.-isopropyl-, methyl ester (Hydrogenated abietic) | 033892-15-8 | 95 |
| 5 | 19.8353 | 3.0007 | Podocarp-7-en-15-oic acid, 13.alpha.-ethyl-13-methyl-, methyl ester (Hydrogenated pimarane-type) | 003827-30-3 | 87 |
| 6 | 19.9317 | 17.084 | Methyl Dehydroabietate (Dehydroabiectic) | 001235-74-1 | 96 |
| 7 | 20.1157 | 0.6982 | Podocarp-7-en-15-oic acid, 13.alpha.-isopropyl-, methyl ester (Hydrogenated abietic) | 033892-12-5 | 83 |
| 8 | 20.3260 | 1.5413 | Methyl abietate (Abietane-type) | 000127-25-3 | 99 |
| 9 | 20.7247 | 0.3640 | Neoabietic acid, methyl ester (Abietane-type) | 003310-97-2 | 90 |
| 10 | 20.8342 | 2.7942 | Merkusic acid, dimethyl ester | 013902-83-5 | 91 |
| 11 | 20.9306 | 0.7811 | Isomer merkusic acid, dimethyl ester* | | |
| 12 | 21.1365 | 1.3093 | Isomer merkusic acid, dimethyl ester* | | |
| | | | **DISPROPORTIONATION PRODUCT at 240 °C (DISPRO240)** | | |
| 1 | 19.1957 | 0.5441 | Sandaracopimaric acid, methyl ester (Pimarane-type) | 001686-54-0 | 99 |
| 2 | 19.3841 | 1.7755 | Podocarp-8(14)-en-15-oic acid, 13.beta.-ethyl-13-methyl-, methyl ester (Hydrogenated pimarane-type) | 003582-27-2 | 87 |
| 3 | 19.5944 | 1.7907 | Isopimaric acid, methyl ester (Pimarane-type) | 001686-62-0 | 98 |
| 4 | 19.7609 | 3.1659 | Podocarp-8-en-15-oic acid, 13.beta.-isopropyl-, methyl ester (Hydrogenated abietic) | 033892-15-8 | 93 |
| 5 | 19.8310 | 1.9825 | Podocarp-7-en-15-oic acid, 13.alpha.-ethyl-13-methyl-, methyl ester (Hydrogenated pimarane-type) | 003827-30-3 | 84 |
| 6 | 19.9186 | 13.4431 | Methyl Dehydroabietate (Dehydroabiectic) | 001235-74-1 | 96 |
| 7 | 20.1114 | 0.8786 | Podocarp-7-en-15-oic acid, 13.alpha.-isopropyl-, methyl ester (Hydrogenated abietic) | 033892-12-5 | 83 |
| 8 | 20.3304 | 0.2973 | Methyl abietate (Abietane-type) | 000127-25-3 | 99 |
| 9 | 20.8342 | 0.5573 | Merkusic acid, dimethyl ester | 013902-83-5 | 91 |
| 10 | 20.9263 | 2.0133 | Isomeric merkusic acid, dimethyl ester** | | |
| 11 | 21.1321 | 1.1285 | Isomeric merkusic acid, dimethyl ester** | | |

* *Peak area percentages represent relative abundances only, since the analysis was conducted by GC–MS without an internal standard or GC–FID quantification.*

***Tentative identification based on interpretation of mass spectral fragmentation patterns*

Among abietane-type acids, methyl abietate (RT 20.338) shows a pronounced decrease in intensity, indicating high reactivity under the applied conditions. The main products detected include methyl dehydroabietate (RT 19.905), associated with dehydrogenation, and peaks at RT 19.765 and 20.115 attributed to hydrogenated abietic-type species. Together, these results indicate that abietic acid undergoes parallel hydrogenation and dehydrogenation pathways, characteristic of disproportionation reactions, with dehydrogenation reported to be the dominant route (Gu et al., 2020; Souto et al., 2011; Wang et al., 2009, 2013).

Neoabietic acid methyl ester (RT 20.724) also decreases markedly after reaction. However, no distinct hydrogenated or dehydrogenated products attributable to neoabietic acid can be clearly resolved by GC–MS. This observation suggests that isomerization to abietic-type structures is the dominant transformation pathway, consistent with earlier reports on Pd/C-catalyzed conversion of neoabietic acid (Wang et al., 2009, 2013).

Dehydroabietic acid methyl ester (RT 19.905), which is already present in the raw material, increases in relative intensity at 200 °C but decreases at 240 °C. At the lower temperature, dehydrogenation appears to proceed more selectively, leading to a higher detectable abundance of methyl dehydroabietate. At 240 °C, increased catalytic

activity likely promotes secondary reactions, including hydrogenation and partial degradation, resulting in a reduced detectable concentration. This trend is consistent with literature reports showing that higher temperatures enhance competing pathways during rosin disproportionation (Souto et al., 2011, 2024).

Merkusic acid exhibits a distinct transformation behavior compared to the other resin acids. The peak of merkusic acid dimethyl ester (RT 20.834) decreases substantially after disproportionation, while two new peaks appear at RT 20.926 and 21.132, indicating the formation of isomeric products.

The mass spectrum of the parent merkusic acid dimethyl ester (Figure 3a, RT 20.834) shows a molecular ion at m/z 364 $[M]^+$, consistent with $C_{22}H_{36}O_4$. A fragment at m/z 333 $[M–31]^+$ corresponds to the loss of a methoxy group, while the base peak at m/z 121 is characteristic of labdane-type diterpenes and is commonly attributed to retro-Diels–Alder-type cleavage of the bicyclic core. This fragment is typically dominant when ring B does not contain a double bond, as the saturated ring facilitates retro-Diels–Alder cleavage leading to a stabilized m/z 121 cation (Azemard et al., 2016). This spectrum serves as a reference for evaluating the transformation products.

For the first isomer (Figure 3b, RT 20.926), the molecular ion at m/z 364 is retained, but the fragmentation pattern changes markedly. The base peak shifts to m/z 175, with a prominent fragment at m/z 235, while the diagnostic m/z 121 ion becomes weak. The m/z 235 fragment corresponds to $[M–129]^+$ and is commonly associated with alkyl side-chain loss in labdane-type diterpenes (Azemard et al., 2016). The marked reduction of the m/z 121 fragment indicates a change in the bicyclic core, consistent with migration of the double bond into ring B, where an endocyclic double bond disfavors the retro-Diels–Alder cleavage responsible for formation of the m/z 121 ion.

The second isomer (Figure 3c, RT = 21.132 min) also retains the molecular ion at m/z 364, but the base peak shifts back to m/z 122, while m/z 175 and m/z 235 appear only as minor fragments. This fragmentation pattern indicates a different isomeric arrangement, while remaining consistent with isomerization of merkusic acid without a change in molecular weight. The observed changes in dominant fragment ions suggest a sequential rearrangement of the double-bond position.

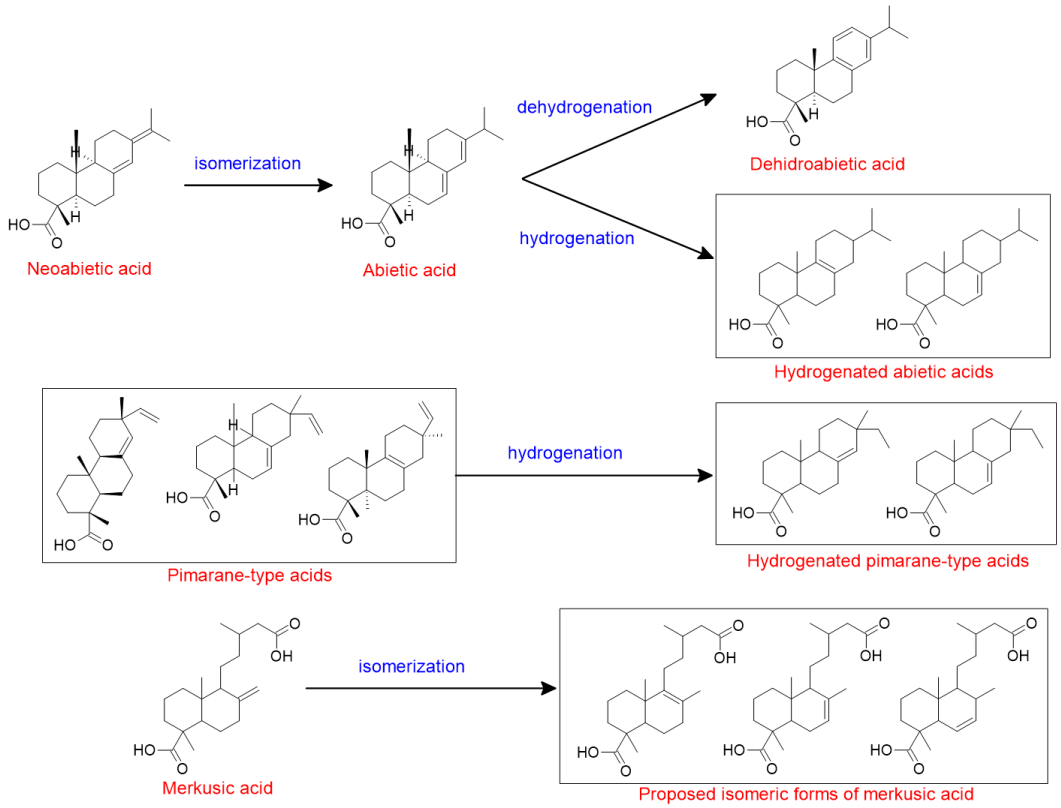


**Figure 4.** Proposed reaction mechanism for the disproportionation, hydrogenation, dehydrogenation, and isomerization of major resin acids over Pd/C catalyst.

Overall, the transformation of merkusic acid during Pd/C-catalyzed disproportionation appears to be dominated by isomerization rather than hydrogenation. This behavior may be related to the structural environment of its double bond. Although the double bond is initially located in an exocyclic position and is therefore prone to migration, the bulky

ISSN: 1410-394X
e-ISSN: 2460-8203

bicyclic framework of merkusic acid is likely to limit effective hydrogenation on the Pd surface. As a result, double-bond migration leading to more stable endocyclic isomers is favored under the applied reaction conditions.

## 4. Conclusions

This study examined the catalytic disproportionation of Indonesian gum rosin over a Pd/C catalyst, with emphasis on the role of merkusic acid. Abietic acid was observed to be among the more reactive resin acids, forming hydrogenated and dehydrogenated products as inferred from GC–MS data. Temperature influenced the observed product distribution, with 200 °C favoring dehydroabietic acid and 240 °C associated with increased hydrogenation and isomerization. Merkusic acid showed a different transformation tendency, with limited evidence of hydrogenation or dehydrogenation and preferential double-bond isomerization. This behavior was indicated by GC–MS peaks with identical molecular ions (m/z 364) but different retention times, together with a shift of the dominant fragment ion from m/z 121 to m/z 175, suggestive of double-bond migration into the bicyclic ring system. These findings provide semi-quantitative, GC–MS-based insight into the temperature-dependent transformation trends of resin acids in Indonesian gum rosin.

**Statement**
During the preparation of this work the authors used ChatGPT 5.2 in order to improve English language and proofread the text. After using this tool/service, the authors reviewed and edited the content as needed and take full responsibility for the content of the publication.

**CRediT authorship contribution statement**
**Meiga Putri Wahyu Hardhianti:** Writing – original draft, review & editing, Visualization, Validation, Resources, Investigation, Formal analysis, Conceptualization.

**Declaration of competing interest**
The authors declare that they have no known competing financial interests or personal relationships that could have appeared to influence the work reported in this paper.

**Data availability**
The data that has been used is confidential.

## References

Azemard, C., Menager, M., & Vieillescazes, C. (2016). Analysis of diterpenic compounds by GC-MS/MS: contribution to the identification of main conifer resins. *Analytical and Bioanalytical Chemistry*, *408*. https://doi.org/10.1007/s00216-016-9772-9

Comyn, J. (1994). Surface characterization of pentaerythritol rosin ester. *International Journal of Adhesion and Adhesives*, *15*, 9–14. https://doi.org/10.1016/0143-7496(95)93637-Z

Gu, Y., Li, Y., Zhang, J., Zhang, H., Wu, C., Lin, J., Zhou, J., Fan, Y., Murugadoss, V., & Guo, Z. (2020). Effects of pretreated carbon supports in Pd/C catalysts on rosin disproportionation catalytic performance. *Chemical Engineering Science*, *216*. https://doi.org/10.1016/j.ces.2020.115588

Hardhianti, M. P. W., Rochmadi, & Azis, M. M. (2022). Kinetic studies of esterification of rosin and pentaerythritol. *Processes*, *10*(1). https://doi.org/10.3390/pr10010039

Hartanto, D. T., Rochmadi, Hardhianti, M. P. W., & Kusumawati, D. (2021). Characteristics and Kinetics Study of Glycerolabietate from Glycerol and Abietic Acid from Rosin. *Jurnal Rekayasa Proses*, *15*(2), 170. https://doi.org/10.22146/jrekpros.69206

Kugler, S., Ossowicz, P., Malarczyk-Matusiak, K., & Wierzbicka, E. (2019). Advances in rosin-based chemicals: The latest recipes, applications and future trends. *Molecules*, *24*(9). https://doi.org/10.3390/molecules24091651

Kumar, R., Chattopadhyay, K., Bhasker, B., Mondal, S., Christopher, J., & Kapur, G. S. (2018). Rapid method for determination of dehydro abietic acid in gum rosin and disproportionate rosin by proton nuclear magnetic resonance spectroscopy. *European Journal of Sciences (EJS)*, 35–42. https://doi.org/10.29198/ejs1804

Ladero, M., de Gracia, M., Trujillo, F., & Garcia-Ochoa, F. (2012). Phenomenological kinetic modelling of the esterification of rosin and polyols. *Chemical Engineering Journal*, *197*, 387–397. https://doi.org/10.1016/j.cej.2012.05.053

Maiti, S., Ray, N., & Kundu, A. K. (1989). Rosin: A Renewable Resource for Polymers and Polymer Chemicals. *Progress in Polymer Science*, *14*, 297–338. https://doi.org/https://doi.org/10.1016/0079-6700(89)90005-1

Mostafalu, R., Heydari, A., Banaei, A., Ghorbani, F., & Arefi, M. (2017). The use of palladium nanoparticles supported on active carbon for synthesis of disproportionate rosin (DPR). *Journal of Nanostructure in Chemistry*, *7*(1), 61–66. https://doi.org/10.1007/s40097-017-0220-y

Pathak, Y. V., & Dorle, A. K. (1987). Study of Rosin and Rosin Derivatives as Coating Materials for Controlled Release of Drug. *Journal of Controlled Release*, *5*, 63–68. https://doi.org/https://doi.org/10.1016/0168-3659(87)90038-1

Silvestre, A. J. D., & Gandini, A. (2008). Rosin: Major Sources, Properties and Applications. In *Monomers, Polymers and Composites from Renewable Resources* (pp. 67–88). Elsevier. https://doi.org/https://doi.org/10.1016/B978-0-08-045316-3.00004-1

Souto, J. C., Yustos, P., Garcia-Ochoa, F., & Ladero, M. (2024). Disproportionation of Rosin Driven by 4,4′-Thio-bis(3-Methyl-6-Tert-Butylphenol): Kinetic

Model Discrimination. *Catalysts*, *14*(4). https://doi.org/10.3390/catal14040235

Souto, J. C., Yustos, P., Ladero, M., & Garcia-Ochoa, F. (2011). Disproportionation of rosin on an industrial Pd/C catalyst: Reaction pathway and kinetic model discrimination. *Bioresource Technology*, *102*(3), 3504–3511. https://doi.org/10.1016/j.biortech.2010.11.022

Tanaka, R., Tokuda, H., & Ezaki, Y. (2008). Cancer chemopreventive activity of "rosin" constituents of Pinus spez. and their derivatives in two-stage mouse skin carcinogenesis test. *Phytomedicine*, *15*(11), 985–992. https://doi.org/10.1016/j.phymed.2008.02.020

Wang, L., Chen, X., Liang, J., Chen, Y., Pu, X., & Tong, Z. (2009). Kinetics of the catalytic isomerization and disproportionation of rosin over carbon-supported palladium. *Chemical Engineering Journal*, *152*(1), 242–250. https://doi.org/10.1016/j.cej.2009.04.052

Wang, L., Chen, X., Sun, W., Liang, J., Xu, X., & Tong, Z. (2013). Kinetic model for the catalytic disproportionation of pine oleoresin over Pd/C catalyst. *Industrial Crops and Products*, *49*, 1–9. https://doi.org/10.1016/j.indcrop.2013.04.015

Wiyono, B., Tachibana, S., & Tinambunan, D. (2006). Chemical Composition of Indonesian Pinus merkusii Turpentine Oils, Gum Oleoresins and Rosins from Sumatra and Java. *Pakistan Journal of Biological Sciences*, *9*, 7–14. https://doi.org/https://doi.org/10.3923/pjbs.2006.7.14

Xu, Z., Lou, W., Zhao, G., Zhang, M., Hao, J., & Wang, X. (2019). Pentaerythritol rosin ester as an environmentally friendly multifunctional additive in vegetable oil-based lubricant. *Tribology International*, *135*, 213–218. https://doi.org/10.1016/j.triboint.2019.02.038

Zhang, D., Zhou, D., Wei, X., Liang, J., Chen, X., & Wang, L. (2017). Green catalytic conversion of hydrogenated rosin to glycerol esters using subcritical CO2 in water and the associated kinetics. *Journal of Supercritical Fluids*, *125*, 12–21. https://doi.org/10.1016/j.supflu.2017.01.009